



# Combined Methods in Preliminary Micro Scale Gas Turbine Diffuser Design – a Practical Approach

M. Czarnecki<sup>1†</sup> and J. Olsen<sup>2</sup>

<sup>1</sup> *Rzeszow University of Technology, Rzeszow, 35-082, Poland*  
<sup>2</sup> *The University of New South Wales, Sydney, N. S. W., 2052, Australia*

†Corresponding Author Email: [czarn@prz.edu.pl](mailto:czarn@prz.edu.pl)

(Received June 29, 2017; accepted December 23, 2017)

## ABSTRACT

Micro scale gas turbines are low cost, simplified versions of full scale jet engines. A unique feature of their design are centrifugal compressor impellers that are selected from automotive low cost, high quality turbocharger components. The present article is dedicated to the practical design of a micro scale centrifugal compressor diffuser that suits a reduced scale, turbojet engine. The idea of using a simplified method comes from the requirement from fast geometry generation for a prototype design. The chosen approach is suitable when the time is crucial and available resources are limited. The chosen simplified analytical model is based on turbomachinery physics. The obtained results are verified by detailed data from successful designs such as KJ66, MW54 and TK50. For a prototype design, GT60 results were compared with a numeric simulation in the ANSYS CFX environment. The difference in isentropic efficiency, numerical prediction in comparison to compressor flow map was less than 3%. This is acceptable for preliminary calculations due to the difference in compressor stator design.

**Keywords:** Centrifugal compressor; Diffuser; Jet Engine; Preliminary design, RC turbine; Turbomachinery.

## NOMENCLATURE

$A$	area	$\Pi$	compression ratio
$b$	impeller blade height	$\eta$	efficiency
$C$	absolute velocity	$\phi_s$	velocity profile lose coefficient
$c$	coefficient		suffixes
$c_p$	specific heat		
$d$	diameter	1	compressor stage inlet cross section (impeller inlet)
$k$	isentropic exponent	2	compressor stage impeller exit cross section
$Ma$	Mach number	3	compressor stage vanned diffuser inlet cross section
$m$	mass flow rate	4	compressor stage vanned diffuser exit cross section static (indexing thermodynamics)
$n$	rotational speed	*	total (indexing thermodynamics)
$n_B$	number of blades	$a$	axial
$p$	pressure	$c$	compressor
$R$	universal gas constant	$cor$	corrected conditions
$r$	radius	$d$	design
$T$	temperature	$dif$	diffuser
$W$	relative velocity	$imp$	impeller
$U$	impeller speed	$in$	inlet
$\alpha$	vane angle	$max$	maximum
$\beta$	backswpt angle	$r$	radial
$\mu$	slip factor		
$\rho$	density		

## 1. INTRODUCTION

Micro gas turbine engines become popular during

the 1990's as a result of the extensive experimental work of Schreckling. To keep the cost of the model low, the gas turbines are manufactured with quality

OEM parts taken from the automotive industry. The compressor impeller is a part that is often shared with gas turbines. The internal layout of turbojet engine requires a different type of diffuser in comparison to a turbocharger design. For an aero engine, the diffuser is required to provide low speed, high pressure flow to the annular combustor. A lightweight, compact design with high pressure recovery is preferred to archive sufficient propulsion efficiency. Low production rates and high R&D cost favors experimental methods that are common to the first generation of micro turbojets. It's a repetitive process of build and test (Schreckling 2000, 2003, 2005; Kamps, 2005). In comparison to commercial diffusers, the micro gas turbine diffuser is downsized to the minimum ratio of 1:5. From a designers perspective all experimental data must be considered with care, due to the fact that most design ratios are not an area of interest for full size solutions (Blevins, 2003; Cohen *et al.* 1996). Another disadvantage is the size of the diffusion channel with a cross section whose average area is 0.00006m<sup>2</sup>. Taking measurements in tiny spaces becomes challenging and expensive. There are two algorithms proposed and applied to test the design (Schreckling 2003; Kamps 2005). In terms of quality they are coupled with engine performance, combustor, axial turbine design, and so inexperienced designers can have difficulties in identifying the proper part of algorithm. Approximately half of the books that discuss micro gas turbine design abandon basic calculations, favoring experiment only (Schreckling 2000, 2005). The proposed calculation method has been used to estimate the initial geometry for the diffuser by the manufacturing company JetPOL since 2014.

## 2. DESIGN CONSIDERATIONS

There are two possibilities to solve this engineering problem:

- design the whole micro gas turbine compressor stage from the beginning by a choosing a impeller and design diffuser, or
- modify the existing solution to improve efficiency making the design simpler and more suitable to produce with less sophisticated equipment.

Starting design from the beginning gives a unique opportunity to study compressor performance maps published by various automotive vendors (BW 2012, HW 2016). Choosing the right compressor impeller for the design is important for the operation of whole engine. It's is best to identify a compressor whose maximum efficiency occurs at a relatively high rotational speed (0.78 – 0.88)  $n_{max}$ . The stage isentropic efficiency should be greater than 72% (Fig. 1). The preferred choice is an impeller with backswept flow channel ( $\beta_2 < 90$ ) rather than a straight one ( $\beta_2 = 90$ ). In general the lower the  $\beta_2$  angle the higher the efficiency and lower the pressure ratio (Cohen *et al.* 1996; Schobeiri 2005).

Modifying the existing design shape is common

practice. This procedure allows matching of engine requirements for suitable airflow and power for stable and self-sustained operation. The impeller from the existing design should be inspected for machining traces (trimming marks) (Parish *et al.* 2000).

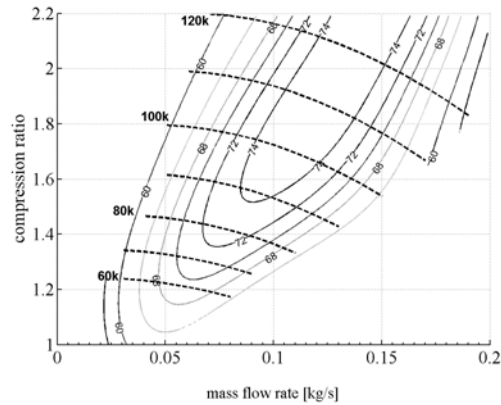


Fig. 1. Example of compressor performance map.

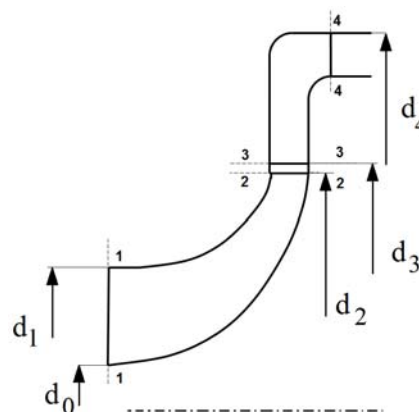


Fig. 2. Diameters important in design compressor stage.

Figure 2 presents important diffuser dimensions. Dimensions  $d_1, d_2, d_3$  are related to given compressor stage impeller. Dimensions  $d_3, d_4$  refer to diffuser. Figure 3 provides information about design velocity triangles.  $C$  is related to the absolute velocity value,  $W$  is a relative to impeller value and  $U$  is an impeller velocity. In terms of applied terminology it is compatible with turbomachinery nomenclature (Cohen *et al.* 1996).

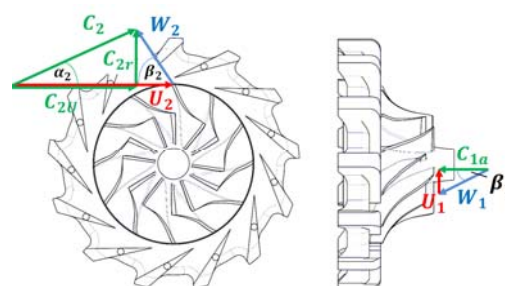


Fig. 3. Velocity triangles required for initial geometry preparation.

The presented design model is a simple and reliable one. The estimated values are useful for preparing the initial CAD geometry and the CFD model for further study. Considering the compressor size, it is important to estimate the compressor parameters based on physics mostly. That is important because more advanced compressor models have built in informal correlations and coefficients that are only suitable for larger size solutions (BLEVINS 2003; ЧУМАКОВ 2009). The presented analytical model is a highly modified version of the design example published in COHEN *et al.* 1996.

## 2.1 Limitations – Impeller Design

For diffuser calculations it is important to identify the mass flow ratio for the compressor (Figs. 2 and 3) due to the risk of a mismatch between the purchased compressor wheel to the compressor flow map (Fig. 1). This often takes place because published compressor maps are mostly for first design or for obsolete designs. The next generations of compressor wheels can have different mass flow ratios, while the OEM reference design number is exactly the same. For example for K24 design, impeller wheel comes with more than three revision from an only one selected supplier. Diameter  $d_1$  differs up to 18.4 %. By an given OEM number it's hard to identify properly compressor performance map (see ZAGE performance catalog). There is required to measure impeller geometry that is characterized by following parameters :  $d_0$  – impeller hub diameter,  $d_1$  – impeller tip diameter,  $d_2$  – impeller external diameter. Additional parameters are:  $\beta_0$ ,  $\beta_1$  – impeller inlet angles,  $\beta_2$  – impeller exit angles (Fig. 3).

The calculations starts from estimating parameters that characterized impeller design. Impeller inlet area is represented by equation :

$$A_1 = \frac{\pi}{4} \cdot (d_1^2 - d_0^2) \quad (1)$$

Impeller outlet area is given by formula :

$$A_2 = \pi \cdot d_2 \cdot b \quad (2)$$

Compressor rotor impeller blade speed at tip and hub for measured diameters  $d_0, d_1, d_2$  are given by equations :

$$U_2 = \frac{\pi \cdot d_2 \cdot n}{60} \quad (3)$$

$$U_1 = U_2 \cdot \frac{d_1}{d_2} \quad (4)$$

$$U_0 = U_1 \cdot \frac{d_0}{d_1} \quad (5)$$

This information is important for selecting the compressor wheel impeller. When the impeller tip speed  $U_2$  is below 450 m/s, then is possible to use a cast compressor wheel. This is a low cost solution; up to 650 m/s, milled compressor impellers are recommended due to their mechanical properties and there ready availability. It's a good practice to

verify high speed impellers by the finite element method (FEM) calculations, but the solver should be a nonlinear one. Note that most of the FEM solvers integrated with CAD systems are linear.

For estimating density of the fluid at impeller inlet is required to known static pressure and static temperature. For selected case values are: static pressure  $p_1=1.013$  [bar], static temperature  $T_1=288$  [K]. In case of designing engine for UAV it's recommended to calculate pressure and temperature values from design flight conditions using ICAO standard atmosphere correlations.

$$\rho_1 = \frac{p_1}{R \cdot T_1} \quad (6)$$

Next step is to estimate the slip factor which reassembles the whirl velocity and inertia forces correlation:

$$\mu = 1 - \frac{0.63 \cdot \pi}{n_{Bimp}} \quad (7)$$

$$\mu = 1 - \frac{\sqrt{\sin \beta_2}}{n_{Bimp}^{0.7}} \quad (8)$$

Slip factor estimated from Stodola correlation Eq. (7) is suitable for a centrifugal compressor with radially tripped impeller blades. The Weisner correlation Eq. (8) is suitable for curved rotor blades. At  $\beta_2 = 90^\circ$ , the difference for a twelve bladed impeller between the Stodola and Weisner correlation is less than 1%.

To predict the impeller mass flow rate, Eq. (9) was applied:

$$m = \frac{\pi^2}{480} [d_1 \tan(\beta_1) + d_0 \tan(\beta_0)] (d_1^2 - d_0^2) \cdot \varphi_s \rho_1 n \quad (9)$$

The inlet speed profile lose factor  $\varphi_s$  is between 0.88 and 0.94 for radial compressor gas turbine applications. A faulty initial mass flow rate prediction manifests itself as a relatively low design efficiency or a failure. When the compressor wheel from an existing engine is considered, it is important to measure the existing geometry because the impeller shape could be trimmed to fit the engine requirements for suitable airflow and power and for stable self-sustained operation (Fig. 2).

To reduce possibilities of human error during geometry translation it is recommended to compare estimated airflow with impellers of similar size (geometry similarity). For compressor performance map estimation corrected airflow parameter is required. The corrected airflow is important factor for compressors. With compressor flow maps, it is possible to read exact values of the overall pressure ratio and process efficiency (compressor maps are usually plotted in “corrected parameters”) for given rotational speed (BW 2012, HW 2016).

Corrected mass flow rate equation is given by formula:

$$m_{cor} = m \cdot \left( \frac{p_h}{p_{1*}} \cdot \sqrt{\frac{T_{1*}}{T_h}} \right) \quad (10)$$

The average axial velocity is found from:

$$C_{1a} = \frac{m \cdot R \cdot T_1}{\rho_1 \cdot A_1} \quad (11)$$

For stage without prewhirl following assumption is true :

$$C_1 = C_{1a} \quad (12)$$

The total pressure and total temperature at the inlet of the compressor is also related to  $C_1$  velocity.

$$T_{1*} = T_1 + \frac{C_1^2}{2 \cdot c_p} \quad (13)$$

$$p_{1*} = \frac{p_1}{\left( \frac{T_1}{T_{1*}} \right)^{\frac{k}{k-1}}} \quad (14)$$

At the impeller eye, the relative velocity is required to check the Mach number. Only  $W_1$  is checked, due to its diameter and tip speed be large in comparison to the impeller eye hub parameters:

$$W_1 = \sqrt{U_1^2 + C_{1a}^2} \quad (15)$$

$$a_1 = \sqrt{2 \cdot \left( \frac{k}{k-1} \right) \cdot R \cdot T_{1*}} \quad (16)$$

$$M_{a1} = \frac{W_1}{a_1} \quad (17)$$

Due to the typical compressor clearance of 0.15-0.2 mm between the impeller and the casing, the Mach number at impeller eye  $M_{a1}$  and at the hub should be below 1.05. If this value is greater than 1.05, then either inlet guide vanes or special bleeding ports like in TJ100 turbojet should be considered.

Engine structure integration is an additional problem that reduces design freedoms. In opposition to commercial gas turbine, micro scale turbine design starts from the internal structure design rather than flow patch design. The mechanical structure depends on machining capability, bearing dimensions, connection points and solving general assembly problem generated by the limited space.

When designing the diffuser, it is important to remember that all joints are over constrained to provide connections free from creep due to the high temperature gradients inside engine core. Blading within the diffuser must allow the installation of connections for fuel, oil and for the ignition system. These items can affect the shape of the blades.

## 2.2 Diffuser Design

General inputs are selected for maximum efficiency (Table 1). Compressor inputs are collected from

original plans (Perish *et al.* 2000; Schreckling 2005). The coefficients  $c_1$  and  $c_2$  are matched with the existing design. As suggested by Schreckling (2003) the coefficient values for  $c_1$  range between 1.04 and 1.09, while for  $c_2$  they range between 1.5 and 1.65 (also see Kamps 2005). Following parameters are related to external diameter of the compressor wheel by equations :

$$d_3 = c_1 \cdot d_2 \quad (18)$$

$$d_4 = c_2 \cdot d_2 \quad (19)$$

The higher  $c_2$  coefficient, allows for better pressure recovery at the diffuser channel by increasing flow cross section area due larger  $d_4$  diameter, however frontal thrust can be seriously decreased by a larger frontal area of the engine (Fig. 2). Collected data for design inputs are presented in table 1.

**Table 1 Design inputs**

	Symbol	Unit	Engine type			
			GT60	TK50	MW54	KJ66
General design inputs (from gas turbine performance data)						
1	n	rpm	120k	130k	135k	95k
2	m	kg/s	0.149	0.092	0.153	0.184
3	$\Pi_c$		2.249	1.849	2.258	1.945
4	$\eta_c$		0.72	0.72	0.72	0.73
Compressor rotor inputs (compressor impeller measurements)						
5	$d_0$	mm	12.5	11	13	13.5
6	$d_1$	mm	38.8	33.5	38.2	46.2
7	$d_2$	mm	60.5	50	54	66
8	b	mm	4,5	4,4	4,5	5
9	$\beta_2$	deg	59	55	85	60
10	$n_{imp}$		12	12	12	12
Compressor diffuser ( design data )						
11	$c_1$		1.075	1.11	1.018	1.08
12	$c_2$		1.586	1.72	1.629	1.627
13	$n_{dif}$		11	11	11	15

For estimating total temperature at compressor exit, it is recommended to know the stage pressure ratio and efficiency. If the compressor map is not available, then as an initial guess, we could use pressure ratios in the range of 1.8 to 3.2. The average compressor isentropic efficiency value chose for this heuristic process is recommended to be between 0.7 and 0.74. It is worth comparing with existing compressors with similar dimensions and trim.

The temperature rise at the compressor stage is estimated from:

$$T_{2*} = T_{1*} \cdot \left[ 1 + \frac{\Pi_c^{(k/k-1)} - 1}{\eta_c} \right] \quad (20)$$

The next step is to estimate the Mach number at the impeller exit is estimated by the following equation:

$$a_2 = \sqrt{2 \cdot \left( \frac{k}{k-1} \right) \cdot R \cdot T_{2*}} \quad (21)$$

When the density  $\rho_1$  is estimated (Eq. 6) it's recommended to check overall compressor pressure ratio is required, i.e.:

$$\Pi_c = \left[ 1 + (k-1) \cdot \eta_c \cdot \mu \cdot \left( \frac{U_2}{a_2} \right)^2 \right]^{\frac{k}{k-1}} \quad (22)$$

The whirl component velocity is given by equation:

$$C_{2U} = \mu \cdot U_2 \quad (23)$$

For initial calculation the choice is recommended (Cohen *et al.* 1996):

$$C_{2r} = C_{1a} \quad (24)$$

and the total absolute velocity  $C_2$ :

$$C_2 = \sqrt{C_{2r}^2 + C_{2U}^2} \quad (25)$$

Static temperature at impeller exit is given by equation:

$$T_2 = T_{2*} - \frac{C_2^2}{2 \cdot c_p} \quad (26)$$

The density at the compressor exit is:

$$\rho_2 = \frac{p_2}{R \cdot T_2} \quad (27)$$

$$M_{a2} = \frac{C_2}{a_2} \quad (28)$$

Due to the simplified nature of these calculations, any result below  $M_{a2} < 1.05$  is considered acceptable. This is because the flow channel of the vaneless diffuser is very shallow and so there is relatively large boundary layer meaning that shock waves do not have the proper conditions to exist.

Total pressure at compressor stage

$$p_{2*} = \Pi_c \cdot p_{1*} \quad (29)$$

Static pressure at compressor stage

$$p_2 = p_{2*} \cdot \left( \frac{T_2}{T_{2*}} \right)^{\frac{k}{k-1}} \quad (30)$$

Density at compressor exit

$$\rho_2 = \frac{p_2}{R \cdot T_2} \quad (31)$$

Radial component of velocity according to impeller geometry

$$C_{2r} = \frac{m}{\rho_2 \cdot A_2} \quad (32)$$

the design angle for the vaneless diffuser:

$$\alpha_2 = a \tan \left( \frac{C_{2r}}{C_{2U}} \right) \quad (33)$$

Since in vaneless diffuser  $C_{2U} = \text{constant}$  for

constant angular momentum (Cohen *et al.* 1996),

$$C_{3U} = C_{2U} \cdot \frac{d_2}{d_3} \quad (34)$$

In designing a vaneless diffuser, due to its very short radial space (2-6 mm), the following assumptions are possible to be applied (Cohen *et al.* 1996)

Knowing impeller channel exit height, instead guessing  $C_{3r}$  radial component value, following assumption was made :

$$C_{3r} = C_{2r} \cdot \frac{A_2}{A_3} \quad (35)$$

and the total absolute velocity  $C_3$ :

$$C_3 = \sqrt{C_{3r}^2 + C_{3U}^2} \quad (36)$$

the design angle for the vane diffuser:

$$\alpha_3 = a \tan \left( \frac{C_{3r}}{C_{3U}} \right) \quad (37)$$

Considering following assumptions when flow channel height at diffuser is constant then  $\alpha_3 = \alpha_2$ .

If diffuser blades has additional construction angle  $\alpha_{db}$  then:

$$\alpha_{3d} = \alpha_3 + \alpha_d \quad (38)$$

The value of the construction angle  $\alpha_d$  varies from -1 up to 2 deg. For designing the final geometry, there are two types of diffuser with a straight blade or a curved one. Straight blades are easy to manufacture and less vulnerable to surge. The disadvantage of straight blades is the smaller pressure recovery. Curved diffuser blades usually give higher performance, with higher pressure recovery at the risk of higher surge due to the narrower gap between the operating line and the surge line (Ling *et al.* 2007).

When designing curved blades, three additional parameters are required for geometry creation, namely the:

Exit design angle given by formula:

$$\alpha_4 = \alpha_{3d} + 10..18^\circ \quad (39)$$

Camber line radius  $r_c$  is described by the equation:

$$r_c = \frac{\left( \frac{d_4}{2} \right)^2 - \left( \frac{d_3}{2} \right)^2}{2 \cdot \left[ \frac{d_4}{2} \cos(\alpha_4) - \frac{d_3}{2} \cos(\alpha_3) \right]}, \quad (40)$$

And the drawing radius  $r_d$  equation:

$$r_d = \sqrt{\left( \frac{d_3}{2} \right)^2 - r_c^2} - \left( \frac{d_3}{2} \right) \cdot r_c \cdot \cos(\alpha_3) \quad (41)$$

Curved diffuser geometry creation is presented on Fig. 4 (Dzygadlo *et al.* 1982).

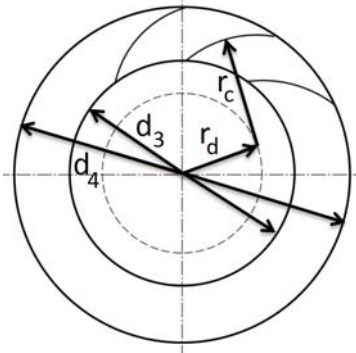


Fig. 4. Curved diffuser geometry creation.

### 2.3. Model Validation

The presented model is verified by real values from the production manual (Perish *et al.* 2000; Schreckling 2005). In terms of verification of the absolute flow angle at the exit of the vaneless diffuser,  $\alpha_3$  was chosen. There is some freedom in representing that angle. For the KJ66 engine, the  $\alpha_3$  angle is measured at the symmetry plane of the diffuser blade. For MW54 positioning plane is from a suction side, while for the TK-50 the positioning is from the pressure side of a blade.

Table 2 Preliminary calculations results

	Symbol	Unit	Engine type			
			GT60	TK50	MW54	KJ66
General design inputs (from gas turbine performance data)						
1	$C_{1a}$	m/s	94.8	78.68	83.6	81.14
2	$W_1$	m/s	261.5	224.7	282.6	243.7
3	$M_1$		0.836	0.72	0.905	0.78
4	$C_{2r}$	m/s	118.76	93.9	112.11	118.3
5	$C_2$	m/s	338.9	278.64	337.89	298.6
6	$M_2$		0.928	0.793	0.926	0.846
7	$C_3$	m/s	315.3	251.63	337.89	276.5
8	$C_4$	m/s	213.7	162	207.42	183.1
9	$\alpha_3$	deg		19.69	19.3	23.34
10	$\alpha_{3d}$	deg	20.5	17.5	19.5	24
11	$\alpha_{4d}$	deg				

For the KJ66, the estimated angle is 23.34 degrees, while the real diffuser had blades at 24 degrees. For the Wren MW54 mk1, the estimated angle is 19.3 degrees, while for the real design, it is 19.5 degrees. For TK50, the estimated angle is 19.69 degrees, while for the real design it is 17.5 degrees as measured from pressure side. Including blade angle real result for TK50 would be close to estimated angle (Table 2). It is common practice to change the estimated angle by couple degrees and is referred as design angle.

The obtained results could be used to estimate the optimal value of design angle by experiment or CFD simulation. In terms of the overall engine design, the compressor section from KJ66 engine is suitable for modification. The inlet velocity  $C_{1a}$  is relatively low compared to other design. The Mach numbers are also lower so there is the

possibility to design new compressor based on impeller obtained from turbochargers. Modern designs based on the same size offers a 50% increase of engine thrust.

## 3. Numerical Computation

### 3.1 Integrated Approach

It is important in design not rely on only one method. For this reason, the data was applied to CATIA V5 CAD system. This system was chosen as a platform for the integration between the results generated by Matlab and the transition platform to the Ansys CFX module. The compressor geometry was reverse engineered from the existing impeller KKK 5324-123-2017. A shared design environment increased productivity greatly. Creating geometry for the fluid simulation requires only adding the external case as a solid body and then extract by means of a Boolean operation (Fig. 5). Other procedures are routine for fluid flow simulation. All operations affect the mechanical design models and the fluid flow model. The mechanical models are:

- the general mechanical concept model (no additional tolerances added – see Fig. 3a),
- the production model (tolerances for manufacturing),
- the fluid domain model (see Fig. 3b)

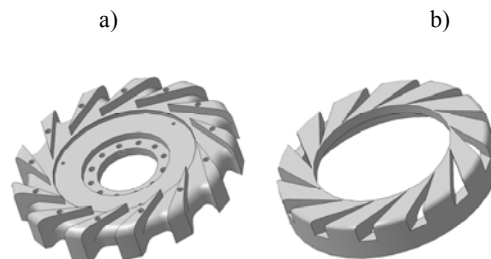
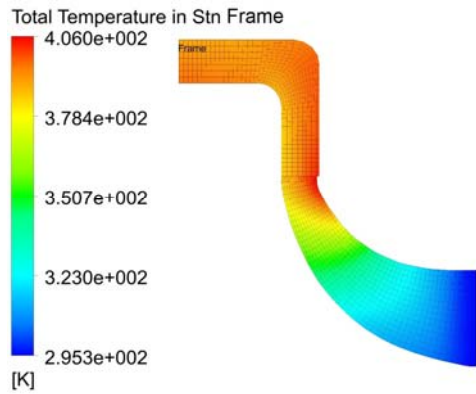


Fig. 5. Integrated design model. a) mechanical model of prototype diffuser b) fluid region model extracted by Boolean operation.

### 3.2 CFD Model

The CFD calculations were made using CFX to get an overall look into the design. The numeric model consists of three domains: the inlet domain (18817 nodes), the rotor domain (169017 nodes), and the stator domain (114511 nodes).

The selected fluid for the simulation was air modelled as an ideal gas with heat transfer based on the total energy model. In terms of turbulence modelling  $k-\epsilon$  was chosen as a suitable for general compressor performance study (industry standard) (Tu, *et al.*, 2012). Additional to this model is the ability to provide reasonable results with a relatively sparse mesh. Boundary conditions applied to the inlet were: total pressure, medium intensity turbulence and static temperature. The boundary conditions at the outlet were: average static pressure with pressure averaging over whole outlet.



**Fig. 6. Meridional surface – total temperature.**

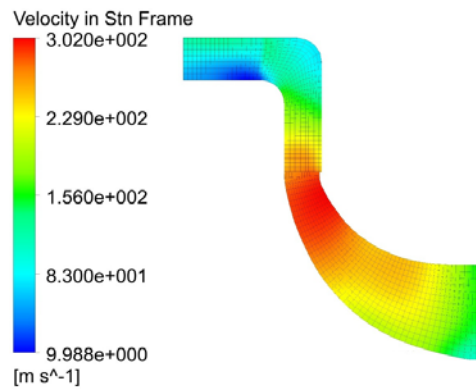


**Fig. 7. Meridional surface – velocity.**

Using a meridional surface (Figs. 6 and 7), it is possible to visualize the velocity vectors of the whole system (rotor/stator). The results correspond to the results presented at table 2 and also reassembles trends that are represented by theory models (Cohen *et al.* 1996).

To verify the design it is important to look at pressure distribution. The static pressure distribution gives information on the pressure recovery at diffuser (Fig. 8). The larger the area of high pressure on the presented figure, the better the pressure recovery at the flow channel.

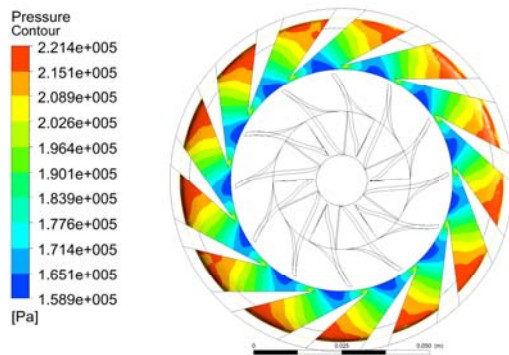


**Fig. 8. Compressor diffuser – static pressure distribution.**

The verified total pressure distribution is a source of information about a flow conditions in crucial

bladeless diffuser (Fig. 9).

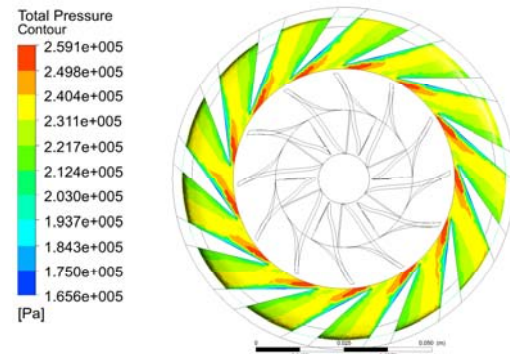


**Fig. 9. Compressor diffuser – total pressure distribution.**

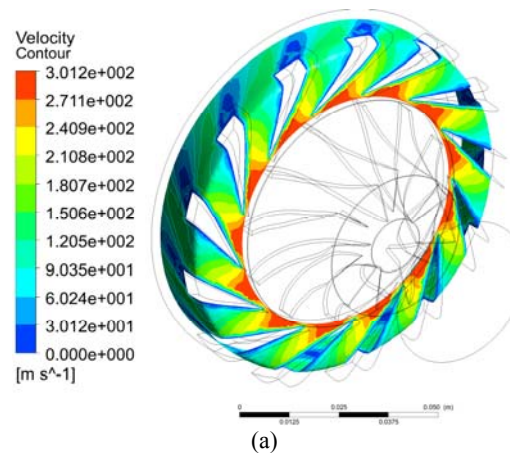


**Fig. 10. Compressor diffuser – velocity distribution. a) front view, b) top view.**

Due to the nature of the pressure flow distribution on the pressure and suction side of diffuser blade presented is not suitable to reach Mach number at the design speed (Fig. 10a). It is possible to increase number of blades but it this should be done with caution. Normally, the number of blades in micro gas turbine diffuser is 11, 13 or 15 blades to avoid resonance with impeller. The velocity contour at the outlet from diffuser suggests that a strong swirling flow enters (Fig. 10b). This swirl has a negative impact on the efficiency that is already reduced by fluid flow friction. A positive impact from swirl is that that reduces the axial velocity component by approximately 30%. It is still a value that is not suitable for combustion.

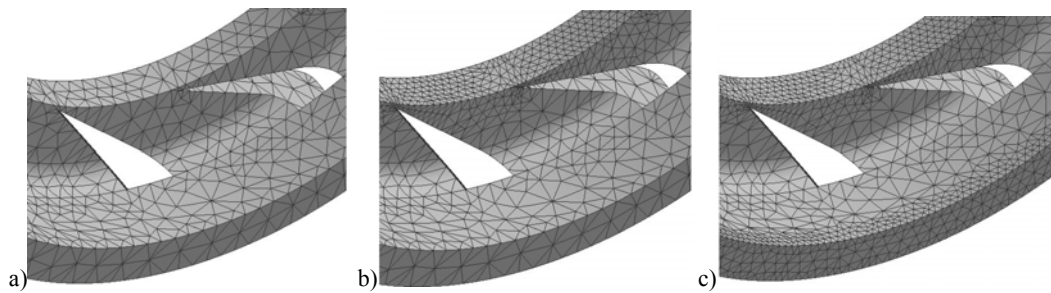


**Fig. 11. Stator fluid domain using different meshing techniques: a) unified mesh, b) decreasing, c) mixed order.**

#### 4. SUMMARY

The presented method of calculating micro gas turbine is simple and provides acceptable results in very short time. Another advantage is that that is not numerically complex. To design a diffuser that matches the impeller, two methods were proposed.

The first produced three diffusers at design angle, design -1 degree, and design +2 degree. Testing the three diffusers allowed us to identify the trend for best efficiency. The advantage of this low cost approach is time saving and lowers the requirements for general engineering skills. This method is recommended for amateur designers who will learn principles of turbomachinery.

The second method of combining an analytical approach and advanced CFD software reduces the time from initial design to working prototype. The simplified model generates geometry that is friendly for any CAD software.

There needs to be caution when working with design modeler (Fig. 11). The three techniques of meshing were tested. A unified mesh is recommended for the initial calculations as it is the most reliable in terms of CAD translation. Increasing or decreasing the order needs user attention in terms of CAD translation especially when there are sharp edges in a fluid domain. It is recommended to replace sharp edges with a surface whose radius is 0.1 mm or less, as that improves reliability and quality of mesh. The mixing density of the mesh in CFX often leads to numerical instabilities using single and double precision solver precision.

Finally the total to total compressor isentropic efficiency for GT60 project needs to be compared. The initial efficiency for compressor stage in analytical model was 0.72 (average value), the efficiency from the compressor flow map was 0.76 (automotive design) and the efficiency estimated by ANSYS CFX turbo mode was 0.738 for the initial simulation. It was not intend to identify optimal efficiency the design angle but to compare results using different tools. Both presented models are suitable for an initial design. The analytical model isentropic efficiency was intentionally under predicted to avoid over prediction in component design. CFD shows that the design has an advantage of 1.8% but is still not as efficient as the

automotive ones. In general CFD gives some possibility to identify the fluid flow distribution even with general turbulence model but the numerical simulation results should be treat as a qualitative. With additional information from engine testing it is possible to obtain best performance out of design.

#### REFERENCES

- Blevins, R. (2003). *Applied Fluid Dynamics Handbook*, Krieger Publishing Company, Melbourne.
- Borg, W. (2012). *Performance turbocharger catalog*. BorgWarner Turbo Systems.
- Cohen, H., G. F. C. Rodgers and H. I. H. Saravanamutto (1996). *Gas turbine theory*. Longman Group Limited, Essex, UK.
- Czarniecki, M. (2014). Reverse Engineering of Centrifugal Compressor Flow Map. *Journal of KONES Powertrain and Transport* 21(4), 57-62.
- Dzygadło, Z. (1982). *Zespoly wirnikowe silnikow turbinowych*. WKL, Warszawa.
- Honeywell (2016). *TBG catalog volume 6*. Honeywell International Inc.
- Kamps, T. (2005). *Model Jet Engines*. Traplet Publications Limited, Worcestershire, UK.
- Ling, J., K. C. Wong and S. Armfield (2007). Numerical Investigation of a Small Gas Turbine Compressor. *16th Australian Fluid Mechanics Conference, Gold Coast, Australia*.
- Parish, R., J. Wright and M. Murphy (2000). *Plans for the MW54 Gas Turbine 2<sup>nd</sup> edition*. Wren Turbines Ltd, UK..
- Schobeiri, M. (2005). *Turbomachinery Flow Physics and Dynamic Performance*. Heidelberg: Springer-Verlag, Berlin, Germany.
- Schreckling, K. (2000). *Model Turbo-Prop Engine for Home Construction*. Traplet Publications Limited, Worcestershire, UK.
- Schreckling, K. (2003). *Gas Turbine Engines for Model Aircraft*. Traplet Publications Limited, Worcestershire, UK.

Schreckling, K. (2005). *Model Turbo-Prop Engine for Home Construction*. Traplet Publications Limited, Worcestershire, UK.

Tu, J., G. H. Yeoh and C. Liu (2012). *Computational Fluid Dynamics : A practical approach*. Elsevier.

ZAGE performance catalog (2014). Taichung City 435, Taiwan R.O.C

ЧУМАКОВ, Ю.А. (2009). Газодинамический расчет центробежных компрессоров

транспортных газотурбинных и комбинированных двигателей. Московский государственный машиностроительный университет (МАМИ), *Gas-dynamic calculations of centrifugal compressors for transport and combined gas turbine engines*. Moscow State Machine-Building University (MAAMI) Moscow, Russia.